BULETINUL Universităţii Petrol – Gaze din Ploieşti	Vol. LX No. 4B/2008	71 -80	Seria Tehnică

Modeling the post combustion monolith catalytic reactor for the carbon monoxide oxidation. Main results

Liviu Filotti, Paul Roşca

"Petroleum & Gas" University of Ploieşti
Petroleum Refining Engineering and Petrochemistry Faculty,
39, Bucharest Blv. / 100520 PLOIEŞTI / Romania
E-mail : lfilotti@upg-ploiesti.ro ; lfilotti@yahoo.com

Abstract

This fourth part of the work covers the results obtained by solving the models of the isothermal or adiabatic monolith converter. Simulated profiles of CO, O_2 reactants concentrations, O_2 excess, bulk gas phase and wall temperatures and reaction rate throughout the monolith length are amongst the main results presented. For a given monolith geometry and feed with known parameters (composition, temperature, pressure, flow rate, close to those of the combustion exhaust from an automobile engine), e.g. *0.6* %vol. *CO and 500* K *, carbon monoxide conversion at monolith outlet reaches 0.9971 for isothermal operation and 0.9997 for adiabatic converter, corresponding to 17.6* ppm *and 1.9* ppm (vol.) *CO concentrations, respectively, at monolith outlet. For the adiabatic converter and same feed, bulk gas temperature grows continuously from the entrance, reaching its maximum value at the monolith outlet, where it is 52.8* K *greater than the feed temperature, while wall temperature decreases from its maximum of 554.4* K *at the entrance to 552.8* K *at monolith exit. The diminution of reaction rate for the adiabatic converter below that for isothermal conditions after roughly one eighth of the monolith length despite higher temperature at wall surface, is due to very low CO concentrations at solid surface in the corresponding sector of the adiabatic monolith. Other quantities (pressure drop, molar concentrations and mole fractions, flow rates, dimensionless numbers Re, Pe, residence time,…) computed using the same steady-state converter models will be presented in a next paper.*

Keywords : *models, monolith, reactor, carbon monoxide, numerical, results*

Main results of monolith converter modelling for the isothermal and adiabatic regimes

The simulation based on the two models, isothermal and adiabatic, were carried out for a converter feed with the parameters specified in Table II-1 (Part II-A [1b]). The primary aim of the simulation was the determination of CO and O_2 reactants concentrations and temperatures profiles throughout the monolith channels. Differential-algebraic equations (DAE) of the models were solved in MathCAD using methods presented in Part III [1c].
For both models used in the present work and in the case of the given set of values for the feed parameters, the reaction rate R_W decreases monotonously, so

$$\frac{dR_{Wi}}{dx} < 0 \ , \ \forall x \in [0, L], i = \text{CO}, \text{O}_2 \ . \tag{1}$$

From previous relation and (I-12) [1a, c] (or from (7), see next) it results that second order derivatives of reactants concentrations with respect to the axial coordinates have only positive values :

$$g_i''(x) > 0 \ , \ \forall x \in [0, L], i = \text{CO}, \text{O}_2 \tag{2}$$

The computed concentrations of carbon monoxide and oxygen (Fig. 1) are indeed positive and continuously decreasing and have positive second order derivatives, respecting thus both conditions (I-22) and (I-23) stated in the first part [1a] as well as the above (2).

The profiles of CO and O_2 gas phase mass molar concentrations along the monolith channels (Fig. IV-1A, B) show a pronounced decline in the first part of the monolith because the catalyzed oxidation reaction is fastest in this zone. The concentrations' drop in the same zone is even steeper for the adiabatic converter (Fig. 1B). The CO (cumulated) conversion, as defined by relation (II-13) (see [1b]), amounts 0.50 (50%) at about 13 *mm* from the monolith entrance in adiabatic regime (total length of the monolith being $L = 150$ *mm*, Table I-1 [1a]), whereas the same conversion is reached after 20 *mm* in isothermal regime.

Computed mass molar concentration of carbon monoxide in the gas phase, g_{CO} , is $0.6065 \cdot 10^{-3}$ *mole CO·kg*$^{-1}$ at converter outlet for the isothermal model and almost ten times lower, *i.e.* $0.0641 \cdot 10^{-3}$ *mole CO·kg*$^{-1}$, for the adiabatic model. The corresponding CO molar fractions at converter outlet, as determined from CO conversions using relation (II-16) [1b], are $17.61 \cdot 10^{-6}$ and $1.86 \cdot 10^{-6}$ respectively. The mentioned CO conversions at the monolith exit are 0.9971 for isothermal converter and 0.9997 for the adiabatic regime. We may also indicate the corresponding computed O_2 conversions, 0.5982 and 0.5998 respectively, but these values are less relevant since oxygen excess is present in the converter feed.

From Fig. 1A, B one may also notice that in the second half of the adiabatic reactor the conversion growth is reduced, the conversion increasing from about 0.98 to the previously mentioned outlet value of 0.9997 only. Such finding lead to the attempts of manufacturing exhaust gas treatment monoliths by techniques allowing fixation on channels walls of a catalyst with different specific activities, smaller in the entrance region and higher in the last part of the monolith. Consequently monoliths having catalysts with low or even zero precious metal content in the entrance region were produced, in order to minimize the consumption of such metals [2] [5a] and improving in the same time monolith tolerance to poisoning [5b].

However, the finishing zone near reactor exit is essential for the achievement of a high conversion, close to 1, and hence of a reduced CO concentration in the treated flue gas. Emissions of carbon monoxide, which is a major pollutant in engine exhaust gases, may therefore comply with stringent standards imposed by the present environmental regulations.

Knowing the computed CO concentration at converter exit, g_{COe} , rough estimations of residual CO amount evacuated into the atmosphere by a vehicle using the simulated converter can readily be made. The (specific) quantity of emitted CO, expressed in *g / km*, the unit preferred by the European or North American standards, can be evaluated following two cases, based on different data :

a) if supposing values for the specific fuel consumption, *Cs*, and the engine air/fuel mass ratio, λ_m , CO emission may be estimated with the simple relation

$$G_{COE} = Cs \cdot (\lambda_m + 1) \cdot g_{COe} \cdot M_{CO} \tag{3}$$

This relation is valid for engine exhaust treatment in the absence of secondary air admission.

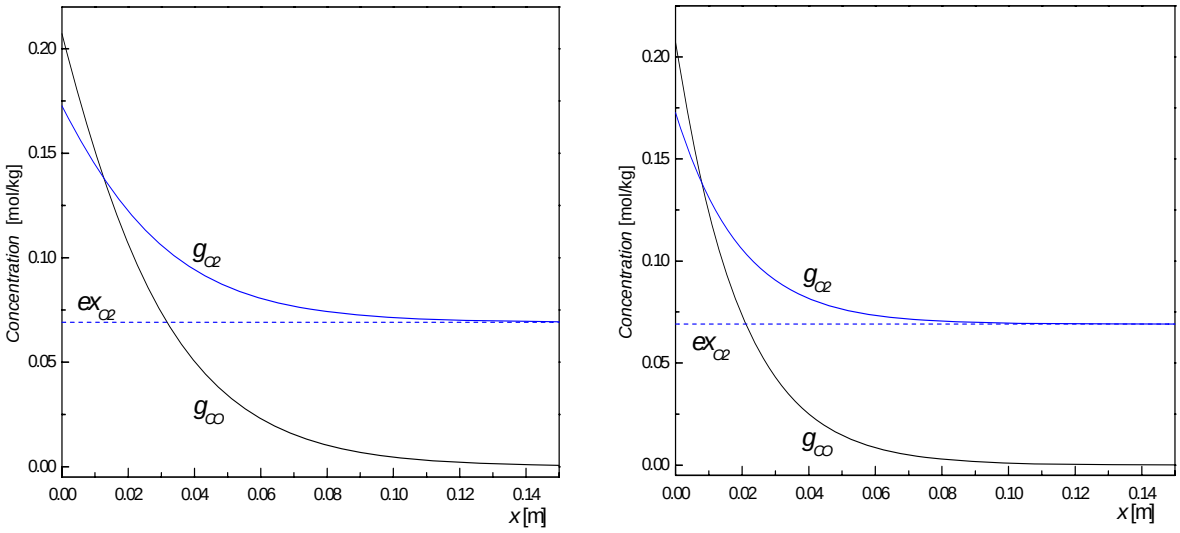

A – isothermal model **B** – adiabatic model

Fig. 1. Computed profiles of mass molar concentrations of CO (g_{CO}), O_2 (g_{O2}) and O_2 excess (ex_{O2}) in the gas phase ($T_0 = 500\ K$, $\Phi = 6$; other parameters as in Tables I-1, II-1 [1a-b])

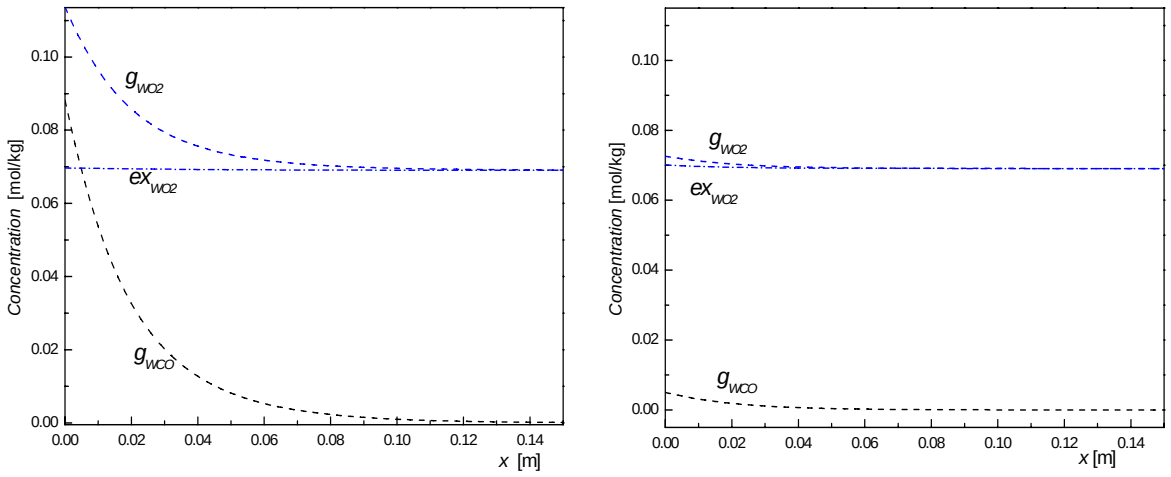

A – isothermal regime **B** –adiabatic regime

Fig. 2. Computed profiles of mass molar concentrations of CO (g_{WCO}), O_2 (g_{WO2}) and O_2 excess (ex_{WO2}) at catalyst surface (in the boundary layer) (same conditions as for Fig. 1 ; concentration scale on the ordinate twice than in Fig. 1)

Considering the average values $Cs = 7.5$ *kg fuel / 100 km* and $\lambda_m = 14.65$ and the computed CO molar concentrations of $0.606 \cdot 10^{-3}$ and $0.064 \cdot 10^{-3}$ *mole* $CO \cdot kg^{-1}$ for converter outlet and reference parameters, emissions rates of $19.9 \cdot 10^{-3}$ and $2.11 \cdot 10^{-3}$ *g CO / km* are estimated with the previous relation for the isothermal and adiabatic regimes, respectively. Note that both CO emission rates thus found are significantly below the limit imposed by Euro IV standard (1 *g CO / km*) [3].

b) if supposing a mean speed of the vehicle, *v*, and with the mass flow rate *G* of the monolith feed already employed as data in the model (see (I-5) and Table II-1 in Parts I, II [1a-b]), carbon

monoxide emission can be calculated with the relation :

$$G_{COE} = \frac{G \cdot g_{COe}}{v} \tag{4}$$

With a mean value v = 40 $km \cdot h^{-1}$, G standard value given in Table II-1 and g_{COe} mentioned above, rates of 1.965 and 0.208 $g\ CO \cdot km^{-1}$ are found for the specific CO emission for the isothermal and adiabatic regimes, respectively. In this more defavorable estimation, the monolith flue gas is complying to the Euro IV standard for CO only in an adiabatic regime, which anyway is the normal operation mode of the monolith.

For the reference set of data used (Tab. II-1, [1b]), in the boundary layer at catalyst surface the O_2 concentration is bigger than CO concentration even at the monolith entrance (Fig. 2) in both regimes, isothermal and adiabatic. For the latter regime, mass transfer coefficients of the two reagents, CO and O_2 , are varying significantly throughout the monolith and have values greater than in isothermal mode, when constant values were admitted for the two coefficients (see relations (II-41), (II-43) in [1b, c]). However, carbon monoxide and oxygen concentrations at catalyst surface, g_{WCO} , g_{WO2} , are significantly lower in adiabatic regime (Fig. 2B), particularly at the monolith entrance, due to a faster consumption of the two reagents than in isothermal mode (Fig. 2A). For example, computed CO and O_2 concentrations in the boundary layer at monolith entrance are 0.088195 and 0.113773 $mole \cdot kg^{-1}$ respectively for the isothermal mode, $4.99617 \cdot 10^{-3}$ and $72.592 \cdot 10^{-3}$ $mole \cdot kg^{-1}$ for the adiabatic regime. In the final zone of the monolith these concentrations get very low values or close to O_2 excess in the gas phase (0.069077 $mole \cdot kg^{-1}$) respectively. Particularly, CO and O_2 concentrations in the boundary layer are for reactor outlet $0.13138 \cdot 10^{-3}$ and 0.069145 $mole \cdot kg^{-1}$ for the isothermal mode, respectively, and $1.6861 \cdot 10^{-6}$ and 0.069078 $mole \cdot kg^{-1}$ in adiabatic regime.
Differences between the reagents concentrations in the gas phase and boundary layer, important especially in the first half of the monolith, prove that diffusion is not negligible and its effect on the global kinetics cannot be ignored.
The CO and O_2 concentrations profiles determined in a previous work [4] based on simpler models of the monolith and using the same data, are for both regimes closed to the profiles determined by the present simulation (Fig. 1, 2).

The O_2 excess is indeed constant in the bulk gas phase for both regimes, isothermal and adiabatic and according relation (III-7) [1c] it is $\kappa/2 = 0.0690771\ldots$ $mole \cdot kg^{-1}$ for monolith feed with the characteristics given in Table II-1 [1b]. In the boundary layer at catalyst surface, O_2 excess (shown in Fig. 3 too) varies along the monolith channels and for both regimes it is greater than O_2 excess in the gas phase, because mass transfer coefficient of oxygen is bigger than that of carbon monoxide.
Oxygen excess in the boundary layer, ex_{WO2} , was calculated with the relation :

$$ex_{WO2} = g_{WO2} - \frac{1}{2} \cdot g_{WCO} \tag{4}$$

It can be also estimated with the relation (5) :

$$ex_{WO2} = \frac{1}{2} \cdot \frac{dg_{CO}(x)}{dx} \cdot \left[F2(x) - F1(x)\right] + \frac{\kappa}{2} \tag{5}$$

equivalent to (4), from which was derived using relations of definition for the two terms $F1$ and $F2$ (III-8a, b) and equations (III-3) and (III-5) [1c]. The last relation (5) is at least as relevant as (4) because it is expressing O_2 excess in the boundary layer as a function of O_2 excess in the bulk gas phase , $\kappa/2$, and reveals the main two phenomena involving the boundary layer : the differentiate diffusion of the two reagents as reflected by the factor [$F2 - F1$] (see meaning of

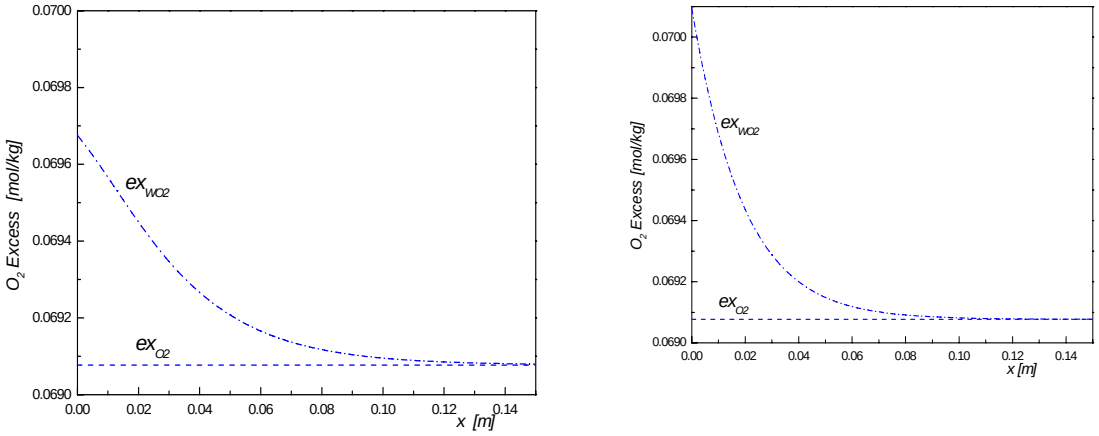

A – isothermal regime **B** - adiabatic regime

Fig. 3. O_2 excess in the gas phase (ex_{O2}) and in the boundary layer (ex_{WO2}) (ordinate scale approx. 120 times greater than in Fig. 1)

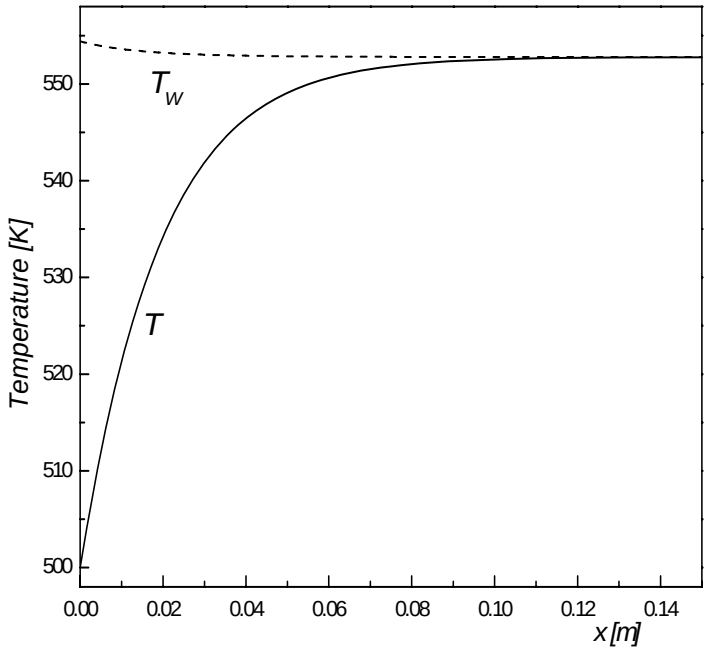

Fig. 4. Gas phase temperature (T) and temperature at catalyst surface (T_W) (adiabatic regime ; same conditions)

terms $F1$, $F2$ given by relations (III-8a, b) [1c]) ; the heterogeneous chemical reaction, by the intermediary of the concentration derivative, dg_{CO}/dx (see also equation (7) below).
Oxygen excess at catalyst surface diminishes from the entrance to the monolith exit, *e.g.* from 0.0696755 to 0.0690795 in isothermal regime or from 0.0700937 to 0.0690774 $mole \cdot kg^{-1}$ in adiabatic regime. As expected, in the exit zone O_2 excess in boundary layer tends to a value equal to the bulk gas phase O_2 excess.

Simulation results show an O_2 excess in the boundary layer in the entrance zone higher for the adiabatic regime than for isothermal mode. Same results also show that for both regimes O_2

excess profiles throughout a monolith channel are similar to the reaction rate profiles. Using (7) (see below), relation (5) can be rewritten :

$$ex_{WO2} = \frac{1}{2} \cdot \frac{a_{cat}}{\Phi} \cdot \left[F1(x) - F2(x)\right] \cdot R_{WCO} + \frac{\kappa}{2} \tag{6}$$

Since parameters a_{cat} , Φ and κ are constant and the difference [$F1$ – $F2$] may be considered approximately constant for the entire monolith channel and having moreover almost the same value for both regimes (actually deviations below 10% according simulation results), it comes that ex_{WO2} presents effectively a profile similar with that of the reaction rate. If admitting mass transfer coefficients profiles for the two reagents CO and O_2 also similar, one can relate the similarity between ex_{WO2} and reaction rate profiles to the stronger sensitivity of the reaction rate to O_2 concentration and to the inhibiting effect of CO. This effect is reflected by the CO concentration (g_{wCO})-containing squared term at the denominator of the LHHW kinetic law (see rate equation (III-1) [1c] or (I-14) and (I-15) [1a]).

Gas phase temperature is increasing continuously from inlet to outlet of the monolith in adiabatic regime. Thus, for a feed with a temperature T_0 = 500 K and the other standard parameters (Table II-1 [1b]), the difference between the outlet and inlet gas phase temperatures is 52.77 K. For the same parameters boundary layer temperature is decreasing continuously along the monolith, from its maximum value at reactor inlet, 554.41 K, to 552.79 K, which value is very close to that of the gas phase temperature at monolith outlet.
The difference between the temperatures of gas phase and catalyst surface is thus most pronounced at the monolith entrance and diminishes gradually towards the exit zone where temperatures tend to become even.
The computed pattern for gas phase temperature (Fig. 4) is close to that determined in a previous work [4] based on a similar but much simpler monolith model (simplified physical and transfer properties estimation, more simplifying assumptions for equations solving,…). On the contrary, there are marked differences between the patterns of the boundary layer temperatures. Preliminary results obtained from simulation with the present model showed that the temperature profile becomes close to that determined in the cited work [4] when the feed temperature is around 485 K. Therefore mentioned differences are probably mainly originating in the different ways used for physical and transport properties estimation in the two works and are not determined by the models equations themselves.

Reaction rates which profiles are represented in Fig. 5A were computed using relation :

$$R_{WCO} = -\frac{\Phi}{a_{cat}} \cdot \frac{dg_{CO}}{dx} \tag{7}$$

which is readily obtained from (I-12) [1a, c]. Reaction rates can be merely determined with the rate law (III-1) [1c] too, resulting thus values very close to those from the relation (7) above. Differences between reaction rates obtained in these two ways are generally much below 4% for the whole monolith length and reach their maximum values near the first third of the monolith length. Details on this behaviour are over the space of the present part of the work, but a short justification is given in the NOTE at the end of the paper.
The two curves in Fig. 5A show a reaction rate in adiabatic regime higher in the first part (first 20 *mm*) of the monolith than in isothermal mode. In the former regime, reaction rate is also decreasing faster along the converter length, down to values smaller than those for isothermal regime. This decrease of the reaction rate in adiabatic regime, despite *a higher temperature at catalyst surface*, is due to the very low CO concentrations in the boundary layer in that portion of the monolith (see also Fig. 2B and 5C-D).

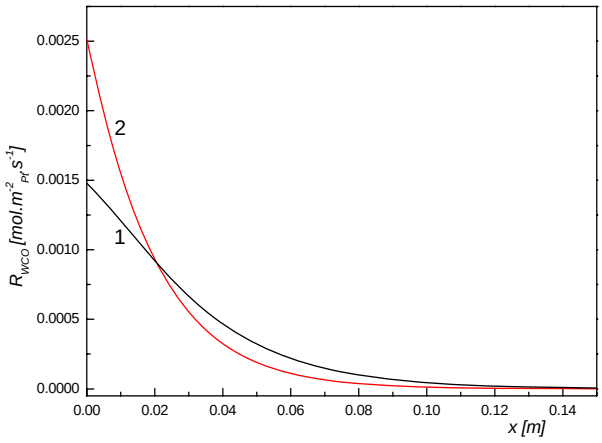

Fig. 5A. Reaction rate along the monolith, isothermal (1) or adiabatic regime (2)

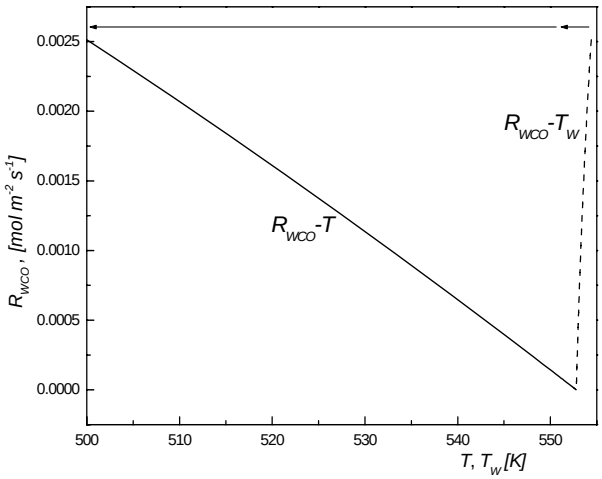

Fig. 5B. Correlation between reaction rate (R_{WCO}) and gas phase temperature (T) or boundary layer temperature (T_W) (adiabatic regime). The arrows show correspondence with the actual reactor axial coordinate and direction of flow through monolith channels (entrance → exit)

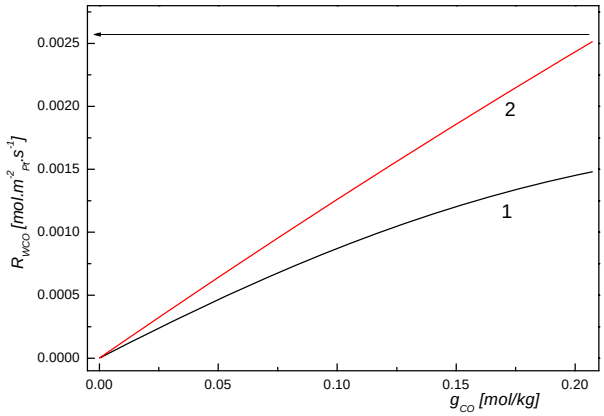

Fig. 5C. Correlations between the computed reaction rates and CO concentrations in the gas phase (g_{CO}), isothermal (1) and adiabatic (2) regimes

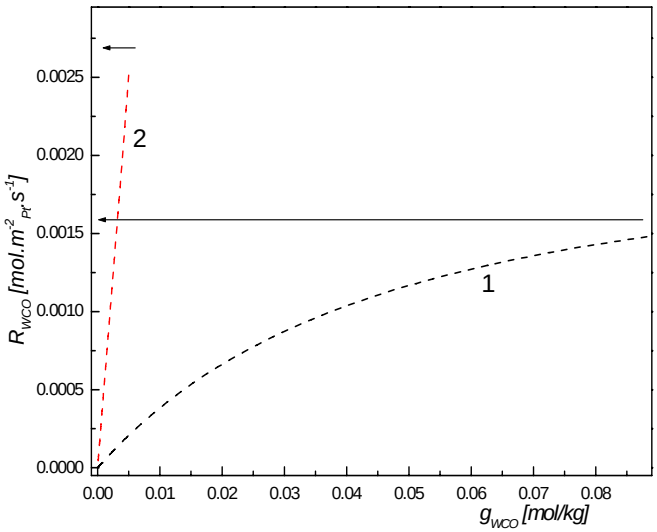

Fig. 5D. Correlations between the computed reaction rates and CO concentrations in the boundary layer (g_{WCO}), isothermal (1) and adiabatic (2) regimes

Reaction rate variations are also reflected by the correlation curves in Fig. 5B : reaction rate decreases along the monolith when the gas phase temperature is greater (within last section of reactor), but it is higher for the *greater temperatures at catalyst surface*.
The curves in Fig. 5 C-D are confirming a reaction rate higher in adiabatic regime than in the isothermal one for same values of CO concentration in the gas phase or in the boundary layer.
It can be also remarked a stronger variation (diminution) of the reaction rate with the CO concentration in the boundary layer than with the CO concentration in the gas phase, in agreement with the contribution of the gas phase-to-boundary layer mass transfer by diffusion of the two reagents. We emphasize that graphical representations of the computed reaction rate as a function of gas phase temperature (T), catalyst temperature (T_W) or CO concentrations (g_{CO} , g_{WCO}) given in figures 5B, C and D are not linear.
The other distributed parameters (molar fractions and concentrations of the components in both gas phase and boundary layer, pressure drop estimation, residence times, dimensionless *Re*, *Pe* numbers,…) of the monolith computed using the same models will be given in the next part.

Conclusion. Perspectives

Catalytic treatment of burnt flue gases is one of the main techniques for the abatement of pollutant emissions resulted from combustion processes. The current paper published in this issue is the fourth part of a series on monolith converter modelling and present the most relevant computed results. At our knowledge, this work is probably the first autochthonous detailed study on monolith reactors modelling.
For simulation of the steady state monolithic reactor 1D (one dimension) models based on equations of mass and heat balances and transfer have been used. Both models, isothermal and adiabatic, have been accounting for the boundary layer at catalyst surface, hence for external diffusion. Values for feed parameters and geometrical characteristics of the monolith were chosen in order to be relevant for automotive catalytic converters [1a-b]. Solving of models equations for both isothermal and adiabatic regimes was made in Mathcad. The main results thus obtained and presented in this fourth part are : mass molar concentrations along the monolith in the gas phase and in the boundary layer for both reagents CO and O_2 , reaction rates, and gas phase and boundary layer temperature profiles (for the adiabatic mode).

For the specified set of data, carbon monoxide (total, or cumulated) conversion is reaching 0.9971 for isothermal mode and 0.9997 for the adiabatic regime, corresponding to a diminution of CO content from 0.207 *mole·kg*$^{-1}$ (molar fraction 0.006) in the monolith feed

down to about $0.61 \cdot 10^{-3}$ $mole \cdot kg^{-1}$ (mole fr. $17.6 \cdot 10^{-6}$) or down to approx. $0.064 \cdot 10^{-3}$ $mole \cdot kg^{-1}$ (mole fr. $1.86 \cdot 10^{-6}$) at monolith exit in the isothermal or adiabatic regime, respectively. In other terms, these values are meaning CO pollutant reduction factors of about 300 and 3000 respectively.

The significant differences found between the computed concentrations of CO and O_2 in the gas phase and in the boundary layer are proving the importance of the diffusion step in both regimes, particularly within the first half of the monolith, where the reagents concentrations are greater and reaction rates also higher.

In the adiabatic mode and for a feed with a 500 K temperature and the other specified parameters, calculated gas phase temperature has its maximum value 552.77 K at monolith outlet, while temperature at catalyst surface (or of the boundary layer) is greatest, 554.41 K, at reactor entrance.

The present study also allowed us to validate the concepts, equations and the solving methods used. Simplified models, with reduced computational demands, may be useful for checks of monolith reactors operating performances. Such models may also turned to profit within software of on-board computers controlling the engine – catalytic converter system.

One of the near-future aims of the study is testing the models and simulation of the converter for various feeds and different geometrical parameters of the monolith. We further intend to improve the models by considering variable dimensionless numbers or the internal diffusion and thermal conduction within the solid. Moreover, our wish is to elaborate an extended model which is applicable to monolith reactors for catalytic combustion, based on tested and herein presented models. Due to higher reagents concentrations, the approximation of physical properties and transfer coefficients (simplifying assumption E [1a]) with independent values on conversion along the monolith is no more valid in the case of catalytic combustion. For the same reason and also due to greater thermal effects, multiple steady states, appearance of light-off zone with sudden variation of converter parameters and failure of conditions (1), (2) are possible for quite large range of feeds [II-9] [II-20]. However, more complex solving (numerical) methods, suited to DAE or PDAE (DAE with partial derivatives) with several solutions with stiff behavior, are needed in order to retrieve the mentioned phenomena from extended model.

NOTE

Differences between reaction rates computed with relation (7) and those calculated with the kinetic equation (III-1) [1c] originate in the reconciliation impossibility of the two relations from the view-point of simplifying assumption E use (see Part I [1a]) : the first relation, (7), employs assumption E only once (for solving the models DAE), while the second relation, (III-1), implies the use of assumption E twice (for solving the models DAE and for the calculation of boundary layer concentrations, g_{WCO} and g_{WO2}, with (III-2) and (III-3)).

LEGEND

(see Parts I, II and III [1a-c] for the rest of symbols)

G_{COE} – (specific) emission of residual CO, $g\ CO \cdot km^{-1}$
Cs – fuel (specific) consumption, 7.5 $kg \cdot km^{-1}$

λ_m – engine air/fuel ratio, 14.65 $kg \cdot kg^{-1}$

References

([I-*n*], [II-*n*] or [III-*n*] in text are sending to the corresponding reference „*n*" cited in Part I, II or III respectively)

1. a) F i l o t t i , L., C î m p e a n u , A., *Buletin UPG - Seria Tehnică*, **LVI** (2004)(No. 4) 94 (Part I) ; b) F i l o t t i , L., *Buletin UPG - Seria Tehnică*, **LVII** (2005)(No. 1) 119, 127 (Parts II-A, II-B) ; c) F i l o t t i , L., *Buletin UPG - Seria Tehnică*, **LVIII** (2006)(No. 3) 39-48 (Part III) ; d) F i l o t t i , L., *Buletin UPG - Seria Tehnică* (Part V, in preparation).
2. a) ASEC, SAE World Congress, 2000, Detroit, SAE Paper 2000-01-0860 ; b) Johnson Matthey, SAE Annual Congress, 1999, Detroit, Papers 1999-01-308, 1999-01-309.
3. *Official Journal of the European Communities* L350, vol. **41** (28 Dec. 1998) ; Directive 98/69/EC.
4. F i l o t t i , L., C î m p e a n u , A., O n u ț u , I., B o h î l ț e a , I., *Rev. Chim. (Bucureşti)*, **54** (2003)(No. 12) 981.
5. T w i g g , M. W., *Platinum Metals Rev*., **45**(2001) (No. 2), 71-73 („Exhaust Emissions Control Developments - A SELECTIVE REVIEW OF THE DETROIT 2001, March 5–8, SAE WORLD CONGRESS").

Modelarea reactorului catalitic de postcombustie cu monolit pentru reacția de oxidare a monoxidului de carbon. Principalele rezultate

Rezumat

Această parte a lucrării cuprinde principalele rezultate obținute cu cele două modele ale convertorului cu monolit în regim staționar, izoterm sau adiabatic, modele ce au fost descrise în detaliu în publicații anterioare [1]. Profilurile calculate ale concentrațiilor reactanților CO şi O_2 şi ale excesului de O_2 , ale temperaturilor în faza gaz şi în stratul limită, precum şi profilul vitezei de reacție de-a lungul monolitului sunt principalele rezultate prezentate. Rezolvarea ecuațiilor diferențial – algebrice ale modelelor a fost făcută în platforma MathCAD [1c]. Parametrii alimentării au fost aleşi astfel încât să fie reprezentativi pentru gaze de ardere de la un motor auto. Pentru o alimentare astfel precizată, cu o concentrație a monoxidului de carbon de 0,6 % (vol.) *şi o temperatură de 500* K*, şi caracteristici constructive ale monolitului date, conversia CO la ieşirea din reactor este 0,9971 în regim izoterm şi 0,9997 în regim adiabatic, corespunzând unei concentrații la ieşirea din reactor 17,6* ppm (vol.) *în regim izoterm şi respectiv 1,9* ppm (vol.) *în regim adiabatic. În regim adiabatic şi pentru aceeaşi alimentare, temperatura fazei gaz creşte continuu, atingând la ieşirea din reactor o valoare cu 52,8* K *mai mare decât cea a alimentării, iar temperatura solidului scade de la valoarea maximă, 554,4* K*, la intrare în reactor, la 552,8* K *la ieşire. Diminuarea vitezei de reacție în regim adiabatic până sub viteza de reacție în regim izoterm după aproximativ o optime din lungimea monolitului, în ciuda unei temperaturi mai mari* la suprafața catalizatorului, *este datorată concentrației foarte mici în regim adiabatic a reactantului CO în stratul limită în porțiunea respectivă a monolitului. Valorile celorlalți parametri distribuiți ce caracterizează funcționarea convertorului, calculate pe baza celor două modele, vor fi prezentate într-un articol ulterior [1d].*